Combined Algebraic Estimator and Extremum Seeking for Estimation of Tire Force and Optimal Slip Ratio ⋆

Henrique C. Mesquita * **Antonio C. Neto** * **Bruno A. Angélico** *
Armando A. M. Laganá *

* *Escola Politécnica, Universidade de São Paulo, SP, (e-mails: henri_came@usp.br, antoniocolombinineto@gmail.com, angelico@usp.br,lagana@lsi.usp.br)*

Abstract: This paper presents an optimal adaptive method for slip ratio optimization in electric vehicles using extremum seeking. The extremum seeking algorithm tracks the optimal slip ratio value that maximizes the tire longitudinal force, which is observed using algebraic estimation. Firstly, a wheel slip control based on a gain-scheduled proportional-integral-derivative controller is proposed. A linearized slip ratio model is developed and utilized to allocate the desired control dynamics, defining the control gains as functions of vehicle speed. Secondly, an algebraic estimator is employed to estimate the longitudinal force applied to the tire, utilizing a gray-box model of the wheel dynamics. Finally, the extremum seeking optimization method is applied to maximize the longitudinal force, a gain dependent on the vehicle speed is proposed to account for disturbances caused by road roughness and imperfections. The results of this application are validated using the CarSim automotive simulator, along with MATLAB/Simulink. The effectiveness of the implemented method is demonstrated for the study case.

Keywords: Adaptive control, slip regulation, tire force estimation, algebraic estimation, extremum seeking

1. INTRODUCTION

In recent years, advances in automotive technology have led to increasingly sophisticated control systems aimed at improving vehicle performance, safety, and efficiency (Chaudhari et al., 2022; You et al., 2022; Wei and Xuexun, 2015). A critical aspect of this endeavor is the real-time estimation and control of key parameters, such as slip ratio and tire forces (Castro et al., 2011; Sunusi et al., 2021; Sado et al., 1999). These parameters exhibit nonlinear behaviors and are sensitive to external disturbances, which can undermine the effectiveness of the control strategy. This issue is particularly evident when accounting for the impact of road irregularities on the system (Cui et al., 2017).

Since these parameters influence vehicle acceleration, optimizing tire forces becomes central to achieving optimal acceleration. This optimization must carefully consider the slip ratio to enhance overall vehicle performance. With this in mind, the utilization of optimization methods in order to determine the maximum value for tire forces is necessary. Various methods have been proposed for this purpose, including recursive square methods (Huang et al., 2017), fuzzy logic (Ding et al., 2018; Gu and Cheng, 2011), and extremum seeking (Zengin et al., 2020; Zhao et al., 2019). The application of recursive square methods is highly dependent on the vehicle model, which, in practice, may exhibit uncertainties and strong nonlinearities. Conversely, to operate effectively across a wide range of conditions, traditional fuzzy logic designs rely on a large set of rules, which can result in higher computational costs. Extremum seeking, on the other hand, has demonstrated excellent results without the high dependence on the vehicle model and lower computational costs, which makes the extremum seeking optimization method a great option for this article.

Even though the choice of applying extremum seeking reduces the model dependency, to optimize the performance, the longitudinal force needs to be used as input to the algorithm. However, its value cannot be measured directly. An alternative is to adopt a gray box model with measurable variables to estimate the longitudinal force on the tire. Many works in this field have used the Kalman filter (Doumiati et al., 2012) and the extended Kalman filter (Reina and Messina, 2019) for real-time estimation of vehicle forces and parameters. While these methods deliver excellent results, they can be costly due to the requirement for expensive optical sensors, as discussed by Liu et al. (2018). Conversely, it has been demonstrated that algebraic estimators exhibit remarkable resilience to disturbances (Fliess et al., 2006; Fliess and Sira-Ramírez, 2008; Aguilar-Ibanez et al., 2021). This is of significant importance to deal with disturbances caused by road conditions and nonlinearities of the system, impacting the tire force and slip ratio. To address these challenges, this article

⋆ The authors thank Fundação de Desenvolvimento da Pesquisa - Fundep Rota 2030 - Linha V, for the Grant VHF-Urbano - Desenvolvimento de um Veículo Urbano Leve Híbrido-Flex, Fundação de Amparo à Pesquisa do Estado de São Paulo - FAPESP, for the Grant 2023/04628-6, and Coordenação de Aperfeiçoamento de Pessoal de Nível Superior - Brasil (CAPES) - Finance Code 001.

employs an algebraic estimator. The developed work can be presented in four distinct steps.

- The design of a gain-scheduled proportional-integral-derivative (GS-PID) control to regulate the slip ratio.
- Development of an algebraic estimator capable of estimating the real-time parameters to be considered in the optimization of the system.
- The optimization of the vehicle acceleration utilizing the extremum seeking method to locate the maximum value for the estimated real-time tire forces to reach the optimized slip ratio.
- Implementation and validation of these algorithms through simulations, demonstrating their effectiveness in improving vehicle acceleration, stability and traction.

This article introduces a method for real-time estimation of the optimal slip ratio by utilizing tire forces and employing adaptive control strategies. The method combines algebraic estimation with extremum seeking optimization to effectively estimate and optimize parameters, showcasing excellent performance even under demanding conditions. Additionally, the study enhances results by incorporating a sigmoid function that depends on vehicle speed. This function helps mitigate the effects of road imperfections, which become more pronounced at higher speeds, a factor often overlooked in most case studies.

In the following sections, the article demonstrates the general modeling, control design strategies, implementation details, simulation results, and conclusions drawn from the study.

2. PROBLEM FORMULATION

The vehicle that is the subject of this article is a passenger electric vehicle with rear-wheel independent drive. A longitudinal vehicle model is used to describe vehicle behavior. The longitudinal equation of motion is expressed as follows:

$$M\dot{v}_x = \sum_i^N F_{x,i} - F_D, \tag{1}$$

where M represents the vehicle mass, v_x denotes the longitudinal speed of motion, and $F_{x,i}$ is the longitudinal tire force on each wheel, with $i = fl, fr, rl, rr$ being an index that identifies the front left, the front right, the rear left, and the rear right wheels, respectively. F_D is the wind drag force over the vehicle, which can be described by

$$F_D = \frac{1}{2}\rho C_d A_f v_x^2, \tag{2}$$

where ρ is the air density, A_f is the frontal area of the vehicle, and C_d is the drag force coefficient.

The tire dynamics is described by a single-wheel model, where the equation of motion is expressed by

$$J_w\dot{\omega}_i = T_i - r_e F_{x,i} \tag{3}$$

where ω_i represents the wheel speed of revolution, J_w denotes the wheel moment of inertia, r_e is the effective rolling radius, and T_i is the drive torque applied to the wheel. In the front wheels, the drive torque is zero and motion is caused only by the longitudinal force. The longitudinal force may be described by

$$F_{x,i} = f(\lambda_i, F_{z,i}) \approx \mu(\lambda_i) F_{z,i} \tag{4}$$

where $F_{z,i}$ represents the normal load over the tire, $\mu(.)$ is a function that models the tire-road friction, and λ_i denotes the tire slip ratio, defined as

$$\lambda_i = -\frac{v_x - r_e\omega_i}{v_x} \tag{5}$$

3. CONTROL DESIGN

3.1 Acceleration Slip Regulation

Let us consider the slip ratio definition provided by (5) and differentiate it over time, yielding the following

$$\dot{\lambda}_i = -\frac{\dot{v_x}\omega_i r_e - v_x\dot{\omega}_i r_e}{v_x^2}. \tag{6}$$

Substituting (1) and (3) into (6) leads to an equation that better models the slip ratio dynamics, expressed as

$$\dot{\lambda}_i = -\frac{r_e}{J_w v_x}\left[r_e F_{x,i} + (1+\lambda_i)\frac{J_w}{M r_e^2}\left(\sum_i F_{x,i} - F_D\right)\right] + \frac{r_e}{J_w v_x} T_i. \tag{7}$$

It should be noted that the coupling between the drive wheels has a relatively minor effect on the slip ratio dynamics, since $\frac{J_w}{Mr_e^2} << 1$. Let us define the auxiliary function

$$\Gamma_i(\lambda_i) = r_e F_{x,i} + (1+\lambda_i)\frac{I_w}{M r_e}\left(\sum_i F_{x,i} - F_D\right). \tag{8}$$

To design a controller capable of stabilizing the wheel slip, (7) should be linearized around the equilibrium point $(\lambda_{i,eq}, T_{i,eq})$. The linear model must meet the constraint $T_{i,eq} = \Gamma(\lambda_{i,eq})$. Linearizing the wheel slip around the equilibrium point and replacing the variables by the input and output deviations of the equilibrium point, defined as

$$\delta\lambda_i = \lambda_i - \lambda_{i,eq}, \qquad \delta T_i = T_i - T_{i,eq}, \tag{9}$$

leads to the first-order differential equation

$$\delta\dot{\lambda}_i = \frac{r_e}{J_w v_x}(-\theta_i\delta\lambda_i + \delta T_i), \tag{10}$$

$$\theta_i = \left.\frac{\partial\Gamma_i}{\partial\lambda_i}\right|_{\lambda_i=\lambda_{i,eq}}. \tag{11}$$

The representation of this transfer function in the Laplace domain, and considering the first-order actuation lag of the electric motor, we arrive at the following linearized transfer function

$$\frac{\Delta\Lambda_i(s)}{\Delta T_{ref}(s)} = \frac{\frac{1}{\theta_i}}{(\tau_m s+1)\left(\frac{J_w v_x}{r_e}\frac{1}{\theta_i}s+1\right)}. \tag{12}$$

Using the linearized slip ratio model provided in (10) it is possible to design a gain-scheduled proportional-integral-derivative (GS-PID) controller to properly regulate the slip ratio. GS-PID gains are scheduled on the vehicle speed and the closed-loop transfer function is represented by the following

$$\frac{\Delta T_{ref}(s)}{\Delta\Lambda_i^*(s) - \Delta\Lambda_i(s)} = K_D(v_x)s + K_P(v_x) + \frac{K_I(v_x)}{s} \tag{13}$$

where K_D, K_I and K_P are the derivative, integral and proportional gain, respectively. The poles of the controlled plant can be expressed by the following equation

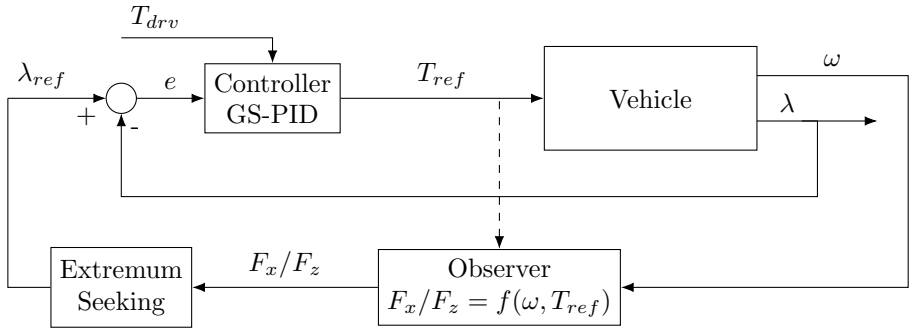

Figure 1. Block diagram of the control scheme

$$s^3+\left\{\frac{1}{\tau_m}+\frac{r_e}{J_w v_x}(\theta_i K_D(v_x))\right\}s^2+\frac{1}{\tau_m}\frac{r_e}{J_w v_x}(\theta_i K_P(v_x))s + \frac{1}{\tau_m}\frac{r_e}{J_w v_x}K_I(v_x)=0. \quad (14)$$

This is a third-order system, which can be designed to have the desired dynamics through pole placement by choosing a fast real pole p_o, a natural frequency ω_n and damping coefficient ξ, so the poles are placed according to the expression

$$(s+p_o)(s^2+2\xi\omega_n s+\omega_n^2)=0. \quad (15)$$

Solving this problem leads to the following conditions for the controller gains:

$$K_I(v) >= \frac{\tau_m J_w v_x p_o \omega_n^2}{r_e}, \quad (16)$$

$$K_P(v) >= \tau_m(2p_o\xi\omega_n+\omega_n^2)\frac{J_w v_x}{r_e}-\theta_{\min}, \quad (17)$$

$$K_D >= \left(p_o+2\xi\omega_n-\frac{1}{\tau_m}\right)\frac{J_w v_x}{r_e}-\theta_{\min}, \quad (18)$$

where $\theta_{\min}$ is the minimum possible value that θ_i might assume. Based on that, we designed a GS-PID in the ideal form $K_P(v)\left(T_D s+1+\frac{1}{T_I s}\right)$ where the gains and the derivative and integral time constants T_D and T_I are those given by Table 1.

Table 1. Parameters of the traction controller

Parameter	Value
$K_P(v)$	$1300v_x+300$
T_D	0.006
T_I	0.04472

3.2 Tire Force Estimation

Algebraic Identifiability Consider a general nonlinear Single-Input Single-Output (SISO) system with a control input $u(t)$ and an output variable $y(t)$. This nonlinear system can be represented by a finite-order ordinary differential equation, which is expressed in the following form:

$$y^{(n)}(t)+a_1 y^{(n-1)}(t)+\cdots+a_n y(t) = b_0 u^{(m)}+\cdots+b_m u(t)+\kappa(t) \quad (19)$$

where $\kappa(t)$ represents structure perturbations acting on the system.

Assumption *1.* The structured perturbation κ can be approximated by a piecewise constant function.

Taking into account Assumption 1, in the Laplace domain the system is written as

$$(s^n+a_1 s^{n-1}+\cdots+a_n)Y(s) = (b_0 s^m+\cdots+b_m)U(s)+\mathcal{I}(s)+\frac{\kappa}{s}, \quad (20)$$

where $\mathcal{I}(s)$ is the polynomial of the initial conditions, of degree $\max(m,n)-1$. Differentiating both sides $\alpha \geq \max(m,n)$ times with respect to s we get rid of the initial conditions, resulting in

$$\frac{d^\alpha}{ds^\alpha}\left\{(s^n+a_1 s^{n-1}+\cdots+a_n)Y\right\} = \frac{d^\alpha}{ds^\alpha}\left\{(b_0 s^m+\cdots+b_m)U\right\}+(-1)^\alpha\alpha!\frac{\kappa}{s^{\alpha+1}}. \quad (21)$$

Isolating κ and taking (21) back to the time domain, it is possible to estimate κ algebraically only with input and output information of the system. Such an estimation will depend on the coefficients a_i with $i=1,\ldots,n$ and b_j with $j=1,\ldots,m$, which do not need to be previously known. Multiplying both sides of (20) by s and then differentiating both sides $\max(m,n)+1 \leq \alpha \leq \max(m,n)+m+n+1$ times with respect to s we eliminate the structured perturbation and the initial conditions, resulting in a linear identifiable equation where a_i and b_j are easily estimated.

Algebraic Force Estimation Consider (3), which describes the dynamics of the wheel. The wheel rotation speed is the system output variable ($y=\omega_i$), the drive torque is the control input ($u=T_i$), and the tire longitudinal force is seen as a disturbance acting on the system ($\kappa=\frac{r_e}{J_w}F_{x,i}$). The system described by (3) may be written as

$$\dot{y}(t)=b_0 u(t)+\kappa, \quad (22)$$

where $b_0=1/J_w$. Transforming (22) into the Laplace domain and then differentiating both sides one time with respect to s yields

$$Y(s)+s\frac{d}{ds}Y(s)=b_0\frac{d}{ds}U(s)-\frac{\kappa}{s^2}. \quad (23)$$

To eliminate derivative terms and smooth noise, both sides are multiplied by s^{-2}, resulting in

$$\frac{1}{s^2}Y(s)+\frac{1}{s}\frac{d}{ds}Y(s)=\frac{b_0}{s^2}\frac{d}{ds}U(s)-\frac{\kappa}{s^4} \quad (24)$$

Note that all terms are of the form $\frac{1}{s^\beta}\frac{d^n}{ds^n}$. Consider the inverse Laplace transform

$$\frac{1}{s^\beta}\frac{d^n}{ds^n}X(s)\leftrightarrow\frac{(-1)^n}{(\beta-1)!}\int_0^t(t-\tau)^{\beta-1}\tau^n x(\tau)d\tau, \quad (25)$$

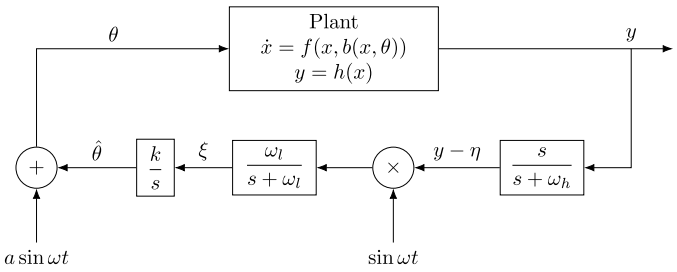

Figure 2. Extremum Seeking Algorithm diagram

equation (24) is transformed back to the time domain

$$\kappa = -\frac{6}{t^3}\int_0^t (t-2\tau)y(\tau)d\tau - \frac{6}{t^3}b_0\int_0^t (t-\tau)\tau u(\tau)d\tau. \quad (26)$$

Taking into account the integration window with duration T and that $\kappa = \frac{r_e}{J_w}F_{x,i}$, resulting in the following expression for the estimated longitudinal force

$$\hat{F}_{x,i} = -\frac{J_w}{r_e}\frac{6}{T^3}\int_0^T (T-2\tau)\omega_i(\tau) + \frac{1}{J_w}(T-\tau)\tau T_i(\tau)d\tau. \quad (27)$$

3.3 Extremum Seeking Algorithm

The extremum seeking scheme is shown in Figure 2. The plant is expressed as

$$\dot{x} = f(x, b(x,\theta)) \quad (28)$$
$$y = h(x) \quad (29)$$

where $b(x,\theta) = u$ represents the control action that stabilizes the plant to the reference θ. The problem of extremum seeking is to find a set point $\hat{\theta}$ that extremizes (maximizes or minimizes) the plant output. The perturbation extremum seeking scheme, shown in Figure 2, allows fast adaptation without prior knowledge of the plant. It searches for a setpoint by adding a sinusoidal perturbation $a\sin\omega t$ to the input of the plant. The high-pass filter eliminates low-frequency signals from the output, the resulting signal is demodulated, multiplying it by the sinusoidal signal $\sin\omega t$. The low-pass filter may not be necessary but is useful for filtering high-frequency components after the demodulation. Thus, through the integrator the optimal setpoint $\hat{\theta} \approx \theta^*$ is estimated.

To properly understand the scheme, consider that the plant varies slowly over time and that the control law is fast enough so that the plant can be viewed as a static map. By applying the Taylor expansion to the output function and neglecting the higher-order terms, the output can be expressed in the following form:

$$y = y^* + \frac{y''}{2}(\theta - \theta^*)^2, \quad (30)$$

where y^* represents the extreme value, and y'' stands for $d^2y/d\theta^2$. Note that $\hat{\theta}$ denotes the estimate of the unknown optimal input θ^*. Let the estimation error be given by

$$\tilde{\theta} = \theta^* - \hat{\theta} = \theta^* - \theta + a\sin\omega t, \quad (31)$$

which, when substituted in (30), gives

$$y = y^* + \frac{y''}{2}(\tilde{\theta} - a\sin\omega t)^2. \quad (32)$$

Expanding this expression and applying the trigonometric identity $2\sin^2\omega t = 1 - \cos 2\omega t$, yields

$$y = y^* + \frac{a^2y''}{4} + \frac{y''}{2}\tilde{\theta}^2 - ay''\tilde{\theta}\sin\omega t - \frac{a^2y''}{4}\cos 2\omega t. \quad (33)$$

The high-pass filter applied to the output removes the constant part y^*. The filter output is then "demodulated" by multiplying $\sin\omega t$, giving the following

$$\sin\omega t\ \frac{s}{s+\omega_h}[y] \approx \frac{y''}{2}\tilde{\theta}^2\sin\omega t - ay''\tilde{\theta}\sin^2\omega t + \frac{a^2y''}{4}\cos 2\omega t\sin\omega t. \quad (34)$$

Applying the trigonometric identity $2\sin^2\omega t = 1 - \cos 2\omega t$ and considering the expression

$$2\cos\omega t\ \sin\omega t = \sin 3\omega t - \sin\omega t, \quad (35)$$

the result signal can be described as

$$\sin\omega t\ \frac{s}{s+\omega_h}[y] \approx -\frac{ay''}{2}\tilde{\theta} + \frac{ag''}{2}\tilde{\theta}\cos 2\omega t + \frac{a^2y''}{8}(\sin\omega t - \sin 3\omega t) + \frac{y''}{2}\tilde{\theta}^2\sin\omega t. \quad (36)$$

The low-pass filter eliminates high frequencies, yielding

$$\xi \approx -\frac{ay''}{2}\tilde{\theta}. \quad (37)$$

Note that $\dot{\tilde{\theta}} = -\dot{\hat{\theta}}$, since θ^* is constant. As $\xi = \frac{\dot{\hat{\theta}}}{k}$, yields that

$$\dot{\hat{\theta}} \approx k\frac{ay''}{2}\tilde{\theta}. \quad (38)$$

As long as $ky'' < 0$ the system is asymptotically stable for $k > 0$ and $y'' < 0$, which means that $\tilde{\theta} \to 0$ and $\hat{\theta}$ converge to a small neighborhood of θ^*.

Algorithm stability The main purpose of the extremum seeking algorithm is to track the maximal longitudinal force, but as demonstrated, the algorithm will only converge to its maximum if $y'' < 0$. The input of the extremum seeking algorithm is the normalized longitudinal force $\mu_i = \frac{F_{x,i}}{F_{z,i}}$, which can be described by the Burckhardt tire model, expressed as

$$\mu_i(\lambda_i) = c_1(1 - e^{-c_2\lambda_i}) - c_3\lambda_i, \qquad \lambda_i >= 0, \quad (39)$$

where $c_1 > 0$, $c_2 > 0$, and $c_3 > 0$ are model parameters. Deriving the model two times with respect to the slip ratio λ_i, yields

$$\mu_i'' = -c_1c_2^2e^{-c_2\lambda_i}, \qquad \lambda_i >= 0. \quad (40)$$

From (40) it is easy to assert that $\mu_i'' < 0$, so the algorithm should convert to the neighborhood of the maximum value.

Implementation Although the extremum seeking should be capable of identifying the value that maximizes the longitudinal force, the algorithm may encounter difficulties in converging to the extremum value if the plant exhibits dynamic behavior or non-Gaussian disturbances at the same frequency as the perturbation of the extremum seeking. The longitudinal force is significantly influenced by imperfections in the road surface, such as roughness and other defects, which are perceived as disturbances. Moreover, the frequency of these disturbances is highly dependent on vehicle speed v_x, as the vehicle gains speed

the disturbance frequency also increases and the road imperfections become more evident.

To ensure that the algorithm remains robust against road disturbances, we define the integrator gain k as a sigmoid function dependent on vehicle speed, expressed as:

$$k = K \cdot \text{sigm}(-(3.6 \cdot v_x - 25)/4) + k_{\min}, \qquad (41)$$

where K and $k_{\min}$ are positive constants. It should be noted that the slip ratio dynamics, as expressed by (7), also depends on the speed of the vehicle. At low speeds, the slip ratio is highly responsive to changes in drive torque, exhibiting rapid variations over time even when a relatively small drive torque is applied. As the vehicle speed increases, the slip ratio becomes progressively less sensitive to the drive torque, as torque changes do not significantly alter the derivative of the slip ratio. As a consequence, if the extremum seeking perturbation has a constant amplitude, the slip controller must progressively increase the drive torque oscillation to follow the reference provided by the extremum seeking. To avoid this, we propose that the perturbation amplitude decreases as the vehicle speed increases, using a perturbation amplitude dependent on the vehicle speed, expressed by

$$a = \min\{a_{\max}, a_{\max}/v_x^{\frac{3}{2}}\}. \qquad (42)$$

Table 2 shows the values of the parameters used in the proposed extremum seeking algorithm.

Table 2. Parameters of the extremum seeking algorithm

Parameter	Value	Unit
ω	100	rad/s
ω_h	90	rad/s
ω_l	10	rad/s
$a_{\max}$	0.015	-
K	39.8	-
$k_{\min}$	0.2	-

4. SIMULATION

To validate the proposed controller, the vehicle was simulated using CarSim, alongside MATLAB/Simulink, where the proposed algorithm was implemented. In the developed test scenario, the vehicle accelerates from standstill on a straight road with a low friction coefficient of 0.5. The driver imposes a fast throttle demand, ramping to full throttle in just 0.5s, so a maximum torque demand is quickly imposed, leading the tire to slip. The vehicle is simulated in two situations, in the first the vehicle rides on a perfect road without imperfections, while in the second the road has imperfections corresponding to a new asphalt overlay.

Simulation on perfect road Figures 3 and 4 show the results of the simulation on the road without imperfections. The longitudinal force rapidly increases, and the proposed algebraic observer estimates the tire longitudinal force almost perfectly, with only a small offset. The algebraic estimator damped some of the oscillations on the longitudinal force, caused by the perturbation of the extremum seeking; however, this was not a problem for the extremum seeking, which converged to an optimal reference, as shown in Figure 4.

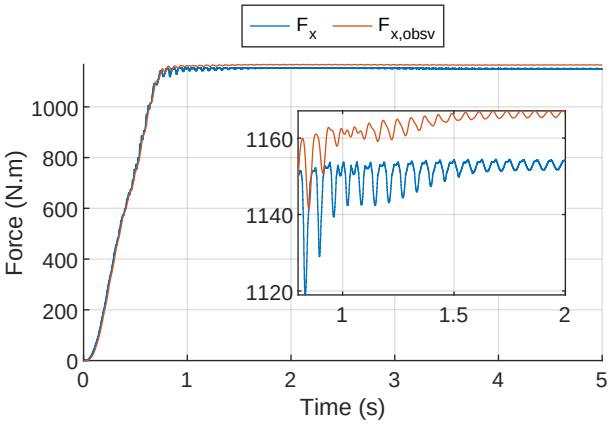

Figure 3. Estimated and simulated tire longitudinal force on the rear left wheel; simulation on perfect road

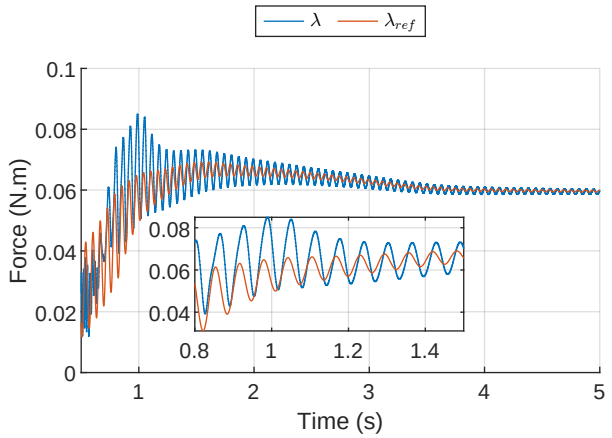

Figure 4. Rear left wheel slip ratio; simulation on perfect road

Figure 4 shows that there is a great error between the reference slip ratio and the actual slip ratio due to the lack of performance of the traction controller and the limits imposed by the motor actuation. Despite this, the extremum seeking high-frequency perturbation still affects the actual slip ratio, being enough for the extremum seeking algorithm to converge.

Simulation considering imperfections Figures 5 and 6 show how the extremum seeking algorithm behaves in a real-world scenario when the road conditions are rough. Figure 5 shows the situation where the integration gain of the extremum seeking algorithm is constant, not varying with the vehicle speed. The estimated optimal slip ratio between the right and left wheels diverges, even if both sides have the same friction coefficient. In contrast, when the integral gain is adjusted according to vehicle speed, the algorithm experiences fewer issues and converges closer to the optimal value, as illustrated in Figure 6

The estimated longitudinal force, shown in Figure 7 still falls close to the real value and captures much of the high-frequency variations. Note that as time passes and the vehicle speed increases, the disturbances affecting the longitudinal force become more pronounced, making it harder to discern the variations caused by the extremum seeking perturbation. This is partly because, as disturbances become more significant, the slip regulator exerts

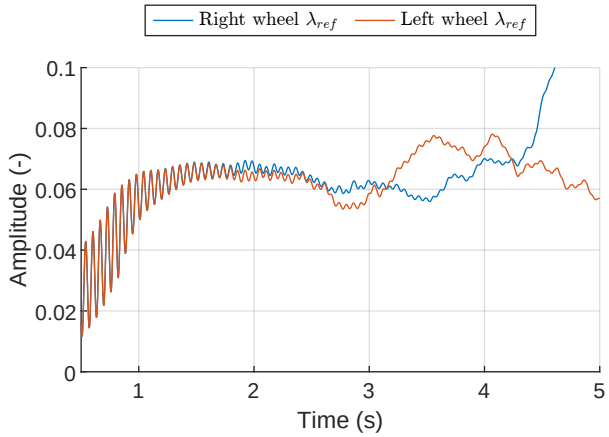

Figure 5. Comparison between the rear right and left wheels slip ratio for constant ESC gain; road with imperfections

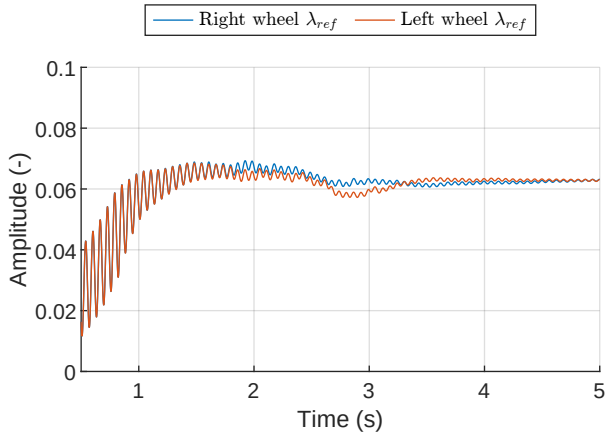

Figure 6. Comparison between the rear right and left wheels slip ratio; road with imperfections

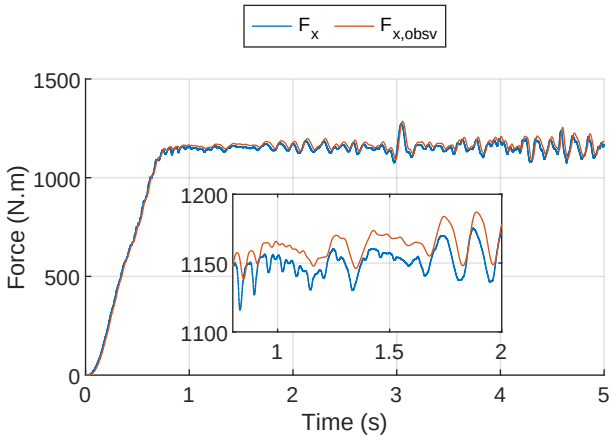

Figure 7. Estimated and simulated tire longitudinal force on the rear left wheel; road with imperfections

greater effort to regulate the slip ratio and compensate for these disturbances, as shown in Figure 8. Due to the disturbances, the slip regulator fails to pass the extremum seeking perturbation to the actual slip ratio.

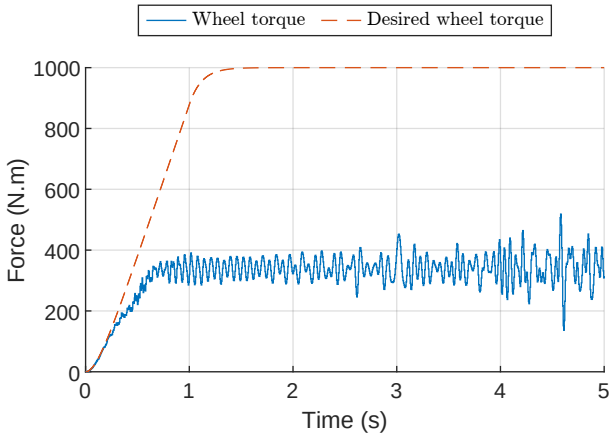

Figure 8. Desired and actual drive torque on the rear left wheel; road with imperfections

5. CONCLUSION

This work presents an adaptive control strategy for slip regulation using tire force estimation. The strategy employs algebraic force estimation for robust parameter estimation, which is resilient to disturbances such as road imperfections. By employing extremum seeking optimization, the method optimizes tire forces to enhance vehicle acceleration and stability. This results in better acceleration with minimal reliance on vehicle models and computational resources. The efficacy of this approach is evident even in challenging conditions such as high-speed driving and varying road surfaces. This is achieved through the integration of a sigmoid function in the optimization process, which reduces the effect of road roughness and other defects in high-speed situations. In conclusion, this study presents a novel real-time approach for estimating and controlling key vehicle dynamics parameters. It offers promising advancements in performance, safety, and efficiency by optimizing acceleration and slip ratio control. Due to its adaptability to varying road conditions and independence from specific vehicle models, it is a viable candidate for automotive control systems.

REFERENCES

Aguilar-Ibanez, C., Sira-Ramirez, H., Acosta, J.Á., and Suarez-Castanon, M.S. (2021). An algebraic version of the active disturbance rejection control for second-order flat systems. *International Journal of Control*, 94(1), 215–222.

Castro, R.D., Araujo, R., and Freitas, D. (2011). Optimal linear parameterization for on-line estimation of tire-road friction. *IFAC Proceedings Volumes*, 44, 8409–8414. doi:10.3182/20110828-6-IT-1002.03220.

Chaudhari, S.D., Shendge, P.D., and Phadke, S.B. (2022). Dynamic nonlinear gradient observer based extremum seeking control for optimum braking. *IEEE Transactions on Industrial Electronics*, 69, 2833–2842. doi:10.1109/TIE.2021.3065612.

Cui, G., Dou, J., Li, S., Zhao, X., Lu, X., and Yu, Z. (2017). Slip control of electric vehicle based on tire-road friction coefficient estimation. *Mathematical Problems in Engineering*, 2017, 1–8. doi:10.1155/2017/3035124.

Ding, X., Zhang, L., Wang, Z., and Liu, P. (2018). Acceleration slip regulation for four-wheel-independently-

actuated electric vehicles based on road identification through the fuzzy logic. *IFAC-PapersOnLine*, 51, 943–948. doi:10.1016/j.ifacol.2018.10.059.

Doumiati, M., Charara, A., Victorino, A., and Lechner, D. (eds.) (2012). *Vehicle dynamics estimation using Kalman filtering: experimental validation*. John Wiley & Sons, Ltd. doi:10.1002/9781118578988.

Fliess, M., Join, C., and Sira-Ramírez, H. (2006). Complex continuous nonlinear systems: Their black box identification and their control. *IFAC Proceedings Volumes*, 39, 416–421. doi:10.3182/20060329-3-AU-2901.00062.

Fliess, M. and Sira-Ramírez, H. (2008). Closed-loop parametric identification for continuous-time linear systems via new algebraic techniques. *Advances in Industrial Control*, 363–391. doi:10.1007/978-1-84800-161-9_13.

Gu, Q. and Cheng, X. (2011). Study on optimal slip ratio identification and traction control for electric vehicle. In *2011 International Conference on Mechatronic Science, Electric Engineering and Computer (MEC)*, 738–742. IEEE. doi:10.1109/MEC.2011.6025570.

Huang, Z., Xu, Z., Chen, B., Zhang, R., Chen, Y., and Peng, Q. (2017). Sliding mode control for urban railway anti-slip system based on optimal slip ratio estimation with forgetting factor recursive least-squares. In *2017 36th Chinese Control Conference (CCC)*, 9502–9507. IEEE. doi:10.23919/ChiCC.2017.8028873.

Liu, J., Peng, Q., Huang, Z., Liu, W., and Li, H. (2018). Enhanced sliding mode control and online estimation of optimal slip ratio for railway vehicle braking systems. *International Journal of Precision Engineering and Manufacturing*, 19, 655–664.

Reina, G. and Messina, A. (2019). Vehicle dynamics estimation via augmented extended kalman filtering. *Measurement*, 133, 383–395.

Sado, H., Sakai, S., and Hori, Y. (1999). Road condition estimation for traction control in electric vehicle. In *ISIE '99. Proceedings of the IEEE International Symposium on Industrial Electronics (Cat. No.99TH8465)*, volume 2, 973–978. IEEE. doi:10.1109/ISIE.1999.798747.

Sunusi, I.I., Zhou, J., Sun, C., Wang, Z., Zhao, J., and Wu, Y. (2021). Development of online adaptive traction control for electric robotic tractors. *Energies*, 14, 3394. doi:10.3390/en14123394.

Wei, Z. and Xuexun, G. (2015). An abs control strategy for commercial vehicle. *IEEE/ASME Transactions on Mechatronics*, 20, 384–392. doi:10.1109/TMECH.2014.2322629.

You, S., Gil, J., and Kim, W. (2022). Fixed-time slip control with extended-state observer using only wheel speed for anti-lock braking systems of electric vehicles. *IEEE Transactions on Intelligent Transportation Systems*, 23, 6368–6378. doi:10.1109/TITS.2021.3055980.

Zengin, N., Zengin, H., Fidan, B., and Khajepour, A. (2020). Slip ratio optimization in vehicle safety control systems using least-squares based adaptive extremum seeking. In *2020 IEEE International Conference on Systems, Man, and Cybernetics (SMC)*, volume 2020-Octob, 1445–1450. IEEE. doi:10.1109/SMC42975.2020.9283109.

Zhao, K., Li, P., Zhang, C., He, J., Li, X., and Liu, J. (2019). Optimal utilization of adhesion force for heavy-haul electric locomotive based on extremum seeking with sliding mode and asymmetric barrier lyapunov function. *Journal of Advanced Transportation*, 2019, 1–15. doi:10.1155/2019/6270515.